

Supporting information for:

Fluvial organic carbon fluxes from oil palm plantations on tropical peatland

Sarah Cook^{1,2*}, Mick J. Whelan², Chris D. Evans³, Vincent Gauci¹, Mike Peacock^{1,4}, Mark H. Garnett⁵, Lip Khoon Kho⁶, Yit Arn Teh⁷, Susan E. Page²

¹ Faculty of STEM, School of Environment Earth and Ecosystems, The Open University, Milton Keynes, MK7 6AA, UK

² Centre for Landscape & Climate Research, School of Geography, Geology and the Environment, University of Leicester, LE1 7RH, UK

³ Environment Centre Wales, Centre for Ecology and Hydrology, Bangor, LL57 2UW, UK

⁴ Department of Aquatic Sciences and Assessment, Swedish University of Agricultural Sciences, 750 07, Uppsala, Sweden

⁵ Natural Environment Research Council Radiocarbon Facility, Rankine Avenue, Scottish Enterprise Technology Park, East Kilbride, G75 0QF, UK

⁶ Tropical Peat Research Institute, Biological Research Division, Malaysian Palm Oil Board, Bandar Baru Bangi 43000, Kajang, Selangor, Malaysia

⁷ Institute of Biological and Environmental Sciences, University of Aberdeen, Aberdeen AB24 3UU, UK

Correspondence to: Sarah Cook (sc606@le.ac.uk)

Contents of this file

1. Figures S1 to S8
2. Tables S1 to S2
3. Text S1 to S2

Introduction

This supplementary material contains the rating curves established using salt dilution gauging for different points in the drainage networks of the Sebungan and Sabaju oil palm plantation. The goodness of fit metrics (R^2) and standard error of the estimate are also provided. The uncertainty associated with the dissolved organic carbon concentrations quantified using the TOC analyser is also provided along with the uncertainty in flux estimates as derived from Monte Carlo Simulations. The annual TOC fluxes for all monitored channels are also provided.

Table S1. Rating curve equations, R^2 and standard error of the estimate for all gauged channels. In all cases y is discharge ($\text{m}^3 \text{s}^{-1}$) and x is stage (m).

Site	Line equation	R^2	Standard error estimate ($\text{m}^3 \text{s}^{-1}$)
SE 1	$y = 0.1167x^{3.3441}$	0.998	0.004
SE 2	$y = 0.1289x - 0.0337$	0.979	0.001
SE 3	$y = 0.0193\ln(x) + 0.0457$	0.956	0.002
SE 4	$y = 0.0719x^{1.5767}$	0.987	0.001
SA 1.2	$y = 0.0675\ln(x) + 0.1231$	0.996	0.001
SA 1.3	$y = 0.1188\ln(x) + 0.14$	0.987	0.004
SA 1.4	$y = 0.0341e^{1.4756x}$	0.954	0.007
SA 3.1	$y = 0.2699x - 0.0406$	0.928	0.026
SA 3.5	$y = 0.0636e^{1.4114x}$	0.957	0.073
SA 3.6	$y = 0.6878x^{2.4519}$	0.978	0.018
SA 4.1	$y = 0.6554x - 0.4501$	0.988	0.015
SA 4.2	$y = 0.0528x^{3.959}$	0.920	0.040
SA 4.3	$y = 0.3919x - 0.3112$	0.941	0.005
SA 4.4	$y = 0.3446x - 0.1165$	0.924	0.020

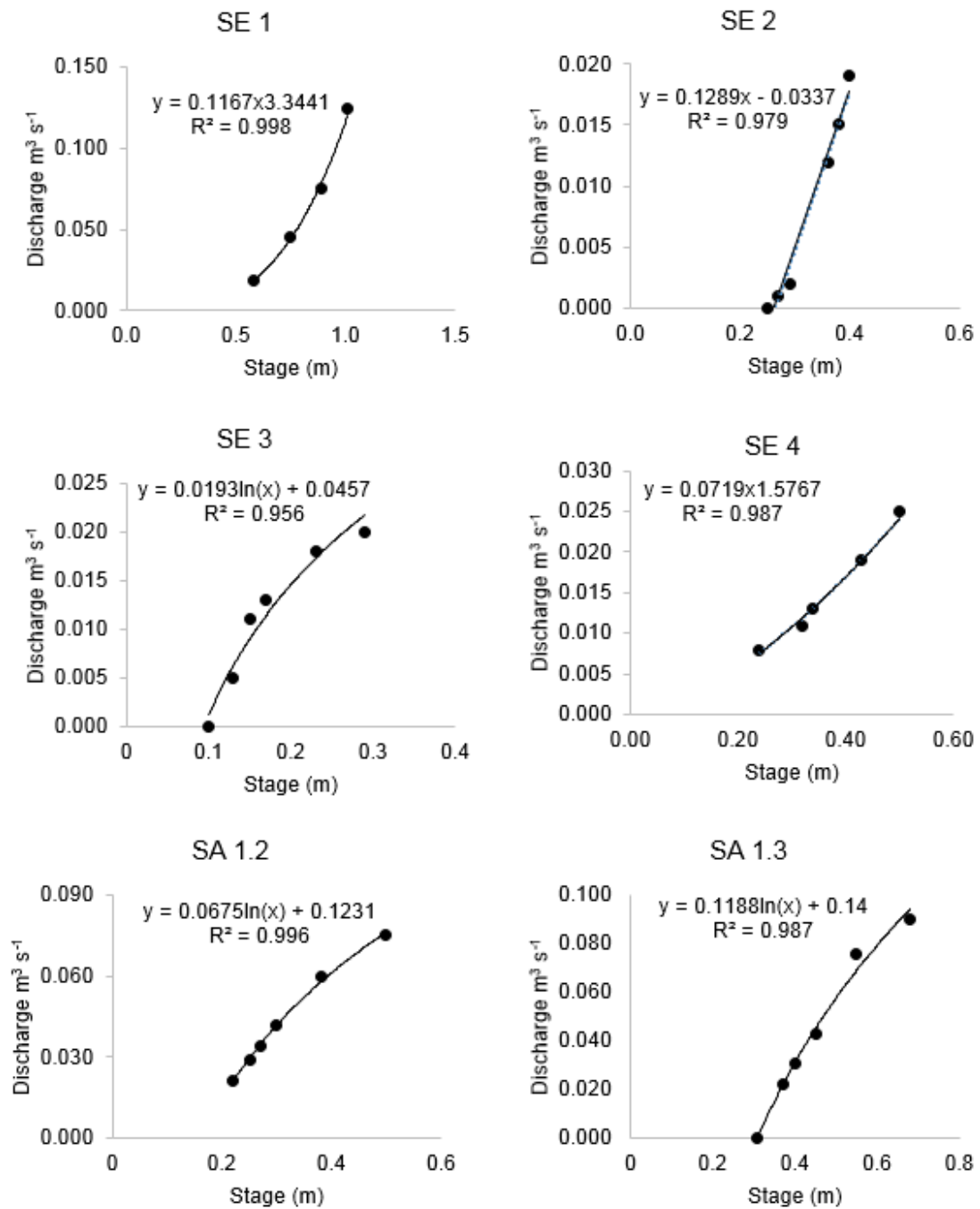


Figure S1. Stage-discharge relationships for drainage channel sites SE 1 to SA 1.3. The equation of best fit and the coefficient of determination (R^2) are also shown.

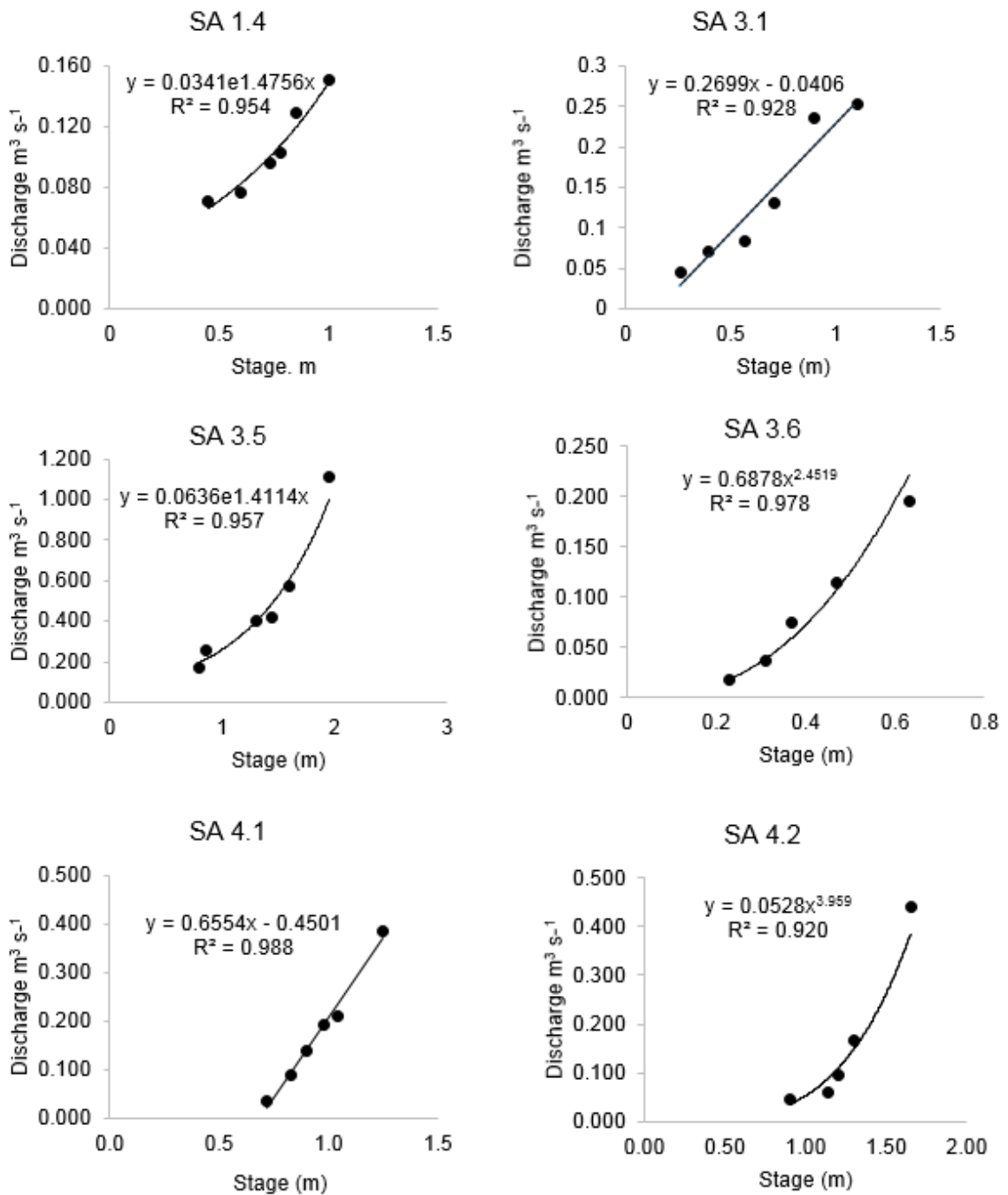


Figure S2. Stage-discharge relationships for drainage channel sites SA 1.4 to SA 4.2.

The equation of best fit and the coefficient of determination (R²) are also shown.

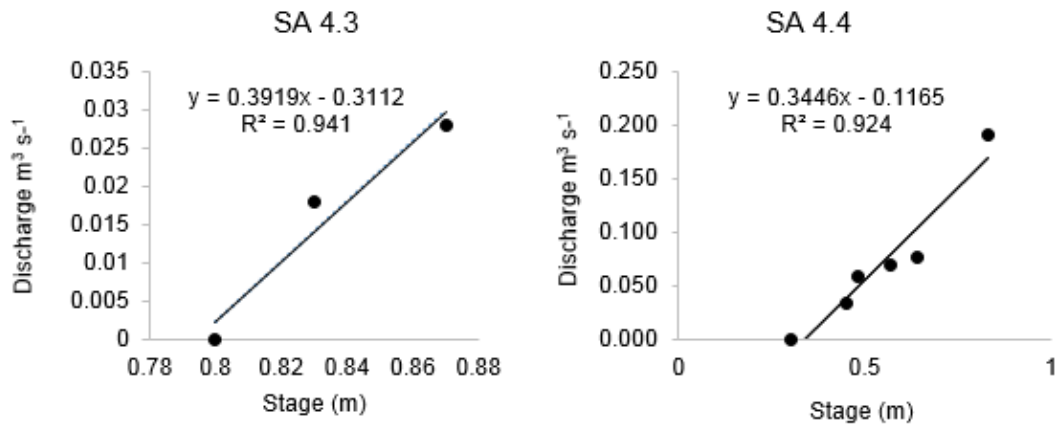


Figure S3. Stage-discharge relationships for drainage channel sites SA 4.3 and SA 4.4.

The equation of best fit and the coefficient of determination (R^2) are also shown.

Text S1

Water samples were analysed on a Shimadzu Total Carbon (TOC) analyser, approximately 12 weeks after collection, and the DOC concentration determined using the non-purgeable organic carbon (NPOC) method. Details can be found in Cook et al. (2016). The standard error for TOC concentrations in the samples ($0.916 \text{ mg C L}^{-1}$) was estimated by inverting the standard error of the estimate of the instrument response (ϵ) in the calibration curve i.e. dividing ϵ by the gradient in the calibration curve (concentration vs response) over a range of standard concentrations between 0 and 100 mg C L^{-1} ($r^2 = 0.998$).

This error estimate is similar to the reported precision (5%) associated with the TOC analyser at concentrations around 20 mg L^{-1} (Graneli et al. 1996; Bjorkvald et al. 2008; Shafer et al. 2010).

Cook et al. (2016) showed that there was no evidence of systematic storage-related DOC loss in the samples, supporting the use of cold storage for DOC preservation.

Text S2

The uncertainty in flux estimates were derived using a Monte Carlo Simulation executed in Microsoft Excel using the @Risk (v7.5) software package (Palisade Corporation, USA). In the estimation of uncertainty about an expected value accounting for covariance is not required. In any case, the extent to which Q_i and C_i are correlated (although variable) is generally not significant. The uncertainty distribution in R_E is shown in Figure S4.

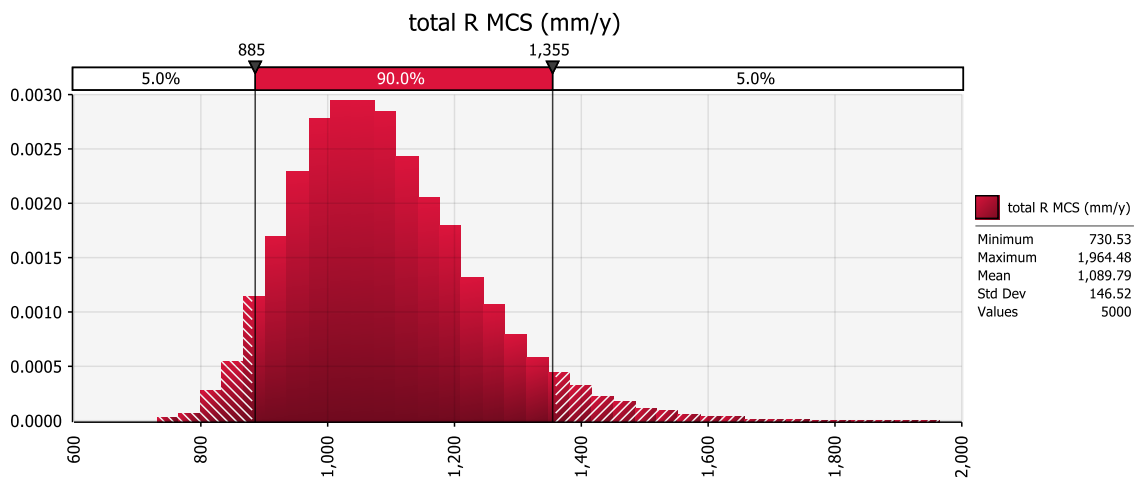


Figure S4. Uncertainty distribution in annual runoff for the study area (mm y^{-1}). Dark shaded area shows the 90% CI.

The uncertainty distribution in J is shown in Figure S5 for SE1, SE2, SE3 and SE4; in Figure 6 for SA1.2, SA1.3, SA1.4 and SA3.1 and in Figure 7 for SA3.5-SA4.4.

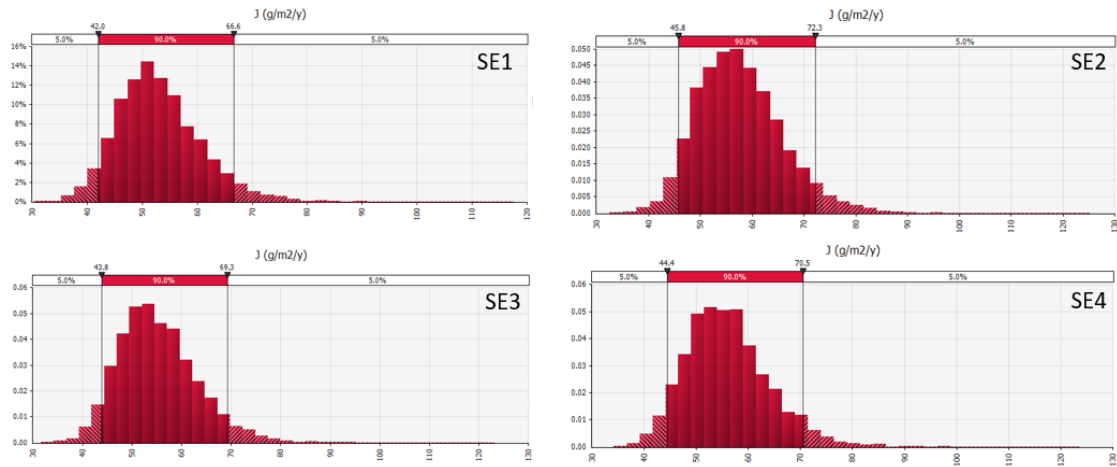


Figure S5. Uncertainty distributions in annual DOC flux estimates for the SE sites ($\text{g m}^{-2} \text{y}^{-1}$). Dark shaded area shows the 90% CI.

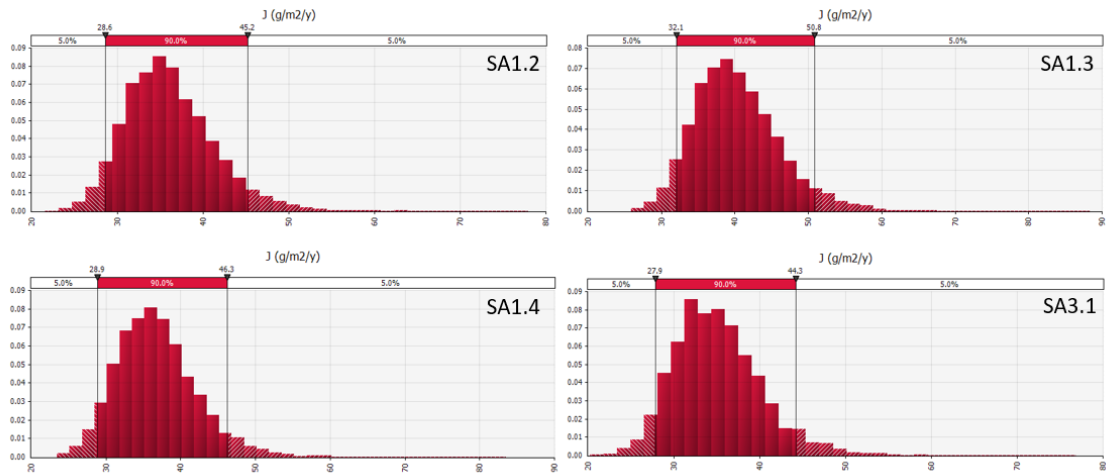


Figure S6. Uncertainty distributions in annual DOC flux estimates for the SA 1.2, 1.3, 1.4 and 3.1 sites ($\text{g m}^{-2} \text{y}^{-1}$). Dark shaded area shows the 90% CI.

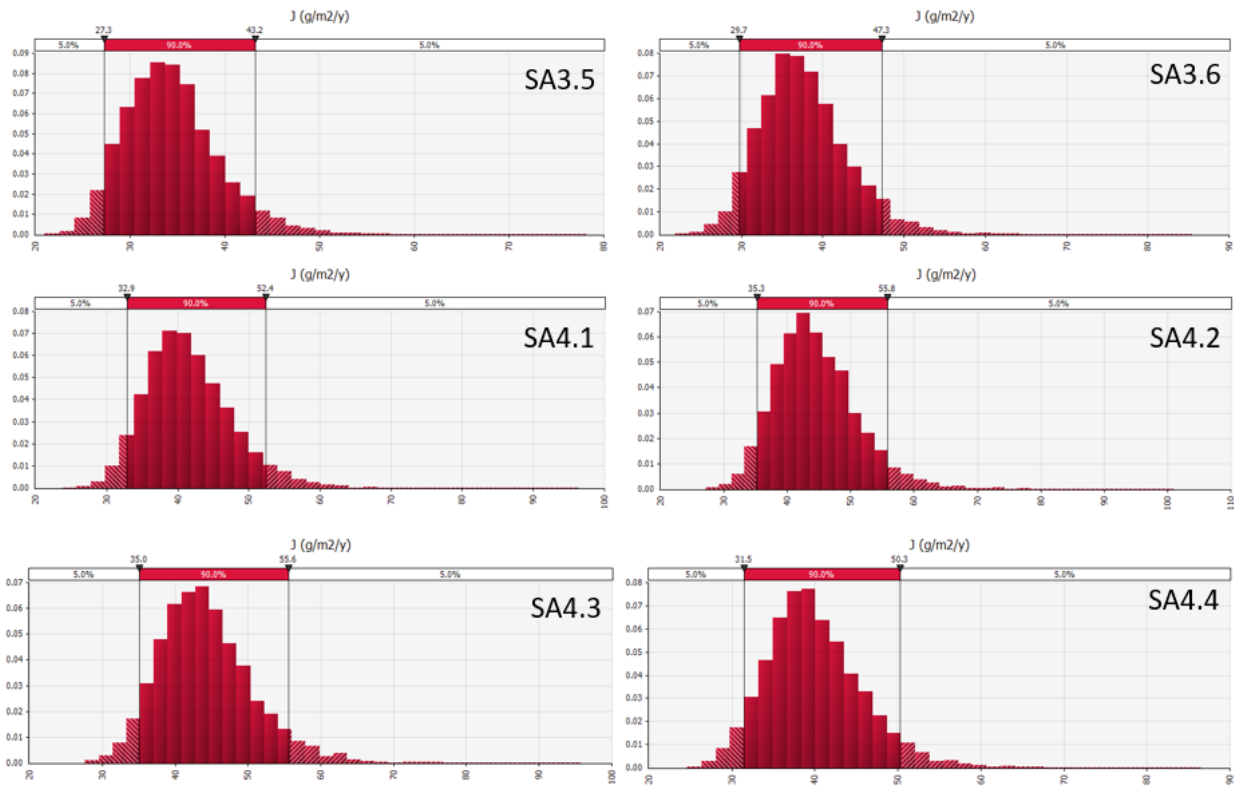


Figure S7. Uncertainty distributions in annual DOC flux estimates for the SA 3.5-4.4 sites ($\text{g m}^{-2} \text{y}^{-1}$). Dark shaded area shows the 90% CI.

Table S2. Annual TOC fluxes, for the individual channels, \pm the 95% confidence interval (CI; standard error \times 1.96) which encompasses the propagated error associated with uncertainty in the DOC concentration, discharge and annual runoff derived from the Monte Carlo Simulation

Site	Mean TOC flux (g C m² yr⁻¹)	\pm 95% CI TOC flux (g C m² yr⁻¹)
SE 1	53.02	14.99
SE 2	57.69	16.25
SE 3	55.22	15.64
SE 4	56.05	15.88
SA 1.2	36.05	10.15
SA 1.3	40.32	11.41
SA 1.4	36.75	10.49
SA 3.1	35.1	9.90
SA 3.5	34.37	9.70
SA 3.6	37.67	10.70
SA 4.1	41.59	11.86
SA 4.2	44.51	12.62
SA 4.3	44.22	12.52
SA 4.4	39.97	11.35